Chaoslike behavior in nonchaotic systems at finite computation precision

Pengliang Shi,[1] Daihai He,[1] Wei Kang,[1] Wujiu Fu,[2] and Gang Hu[3,1]
[1]*Department of Physics, Beijing Normal University, Beijing 100875, China*
[2]*Department of Physics, Fuzhou Normal College, Jiangxi Province 344000, China*
[3]*Center of Theoretical Physics, Chinese Center of Advanced Science and Technology (World Laboratory), Beijing 8730, China*
(Received 25 August 2000; published 29 March 2001)

The dynamical behavior of a two-dimensional map is investigated numerically. A chaoslike behavior, i.e., a nonsmooth distribution of the attractor and seemly sensitive dependence of the motion on initial condition is found as the system state is nonchaotic (both Lyapunov exponents are nonpositive). The key point for this strange behavior is that the mode corresponding to the second negative Lyapunov exponent contains positive local Lyapunov exponent segments. It is argued that this kind of behavior may be typical and easily observed in practical numerical computations and experiments where small noise is inevitable.

DOI: 10.1103/PhysRevE.63.046310 PACS number(s): 05.45.−a

I. INTRODUCTION

It is well known in the study of chaos that Lyapunov exponents (LEs) play an important role in characterizing the dynamics of chaotic system. In particular, the positive largest LE is the key feature for describing the sensitive initial-condition dependence of the chaotic motion [1–4]. Recently, negative LEs, which contain some positive local Lyapunov segments, have attracted more and more attention. For instance, in quasiperiodically forced systems with strange nonchaotic attractors (SNA), the two trivial largest LEs are zero, and the third LE is negative which, however, plays the crucial role in determining the features of SNA, the importance of this point was emphasized in Refs. [5,6]. The shadowing problem of chaotic systems was discussed in Refs. [7–12]. It was clear that the shadowing of chaotic trajectories may be broken if the second negative LE of a two-dimensional map (suppose the system has a single positive LE) contains local positive LE. It is interesting to further explore the new characteristic features of the system dynamics brought by such negative LEs with positive segments of local LE.

In a LE spectrum, the largest LE has been computed most frequently. There are two computation methods conventionally accepted which are regarded to be equivalent. The first method is to compute the divergence rate of two adjacent trajectories of the system, the distance between the two trajectories is frequently reset to a constant, which is much smaller than the attractor scale and much larger than the computation error, namely

$$\lambda_1(D)=\lim_{t\to\infty}\frac{1}{t}\sum_{n=1}^{t}\ln\Delta l_n(D)-\ln\Delta l_0(D), \qquad (1)$$

where $\lambda_1(D)$ is the largest LE of the system, $\Delta l_n(D)$ is the distance after nth iteration while $\Delta l_0(D)$ is the distance to which we reset $\Delta l_n(D)$ before each iteration and after the previous iteration. The second one is to work in the tangent space of the dynamic system. For a q-dimensional system, f: $R^q\to R^q$, with the trajectory $X_{n+1}=f(X_n)$, $n=0,1,2,\ldots$, there are q exponents which are customarily ranked from the largest to the smallest $\lambda_1(T)\geqslant\lambda_2(T)\geqslant\cdots\geqslant\lambda_q(T)$. Associated with each exponent $j=0,1,2,\ldots,q$, there are nested subspaces $V^j\in R^q$ of dimension $q+1-j$ and with property that

$$\lambda_j(T)=\lim_{t\to\infty}\frac{1}{t}\ln\|(Df^t)_{X_0}\cdot v_j\| \qquad (2)$$

for all $v_j\in V^j\setminus V^{j+1}$. Notice that for $j\geqslant 2$ the subspaces V^j are sets of Lebesgue measure zero, and so for almost all $v\in R^q$ the limit in Eq. (2) equals $\lambda_1(T)$. Since $(Df)^t_{X_0}=(Df)_{X_t}\cdot(Df)_{X_{t-1}}\cdot\cdots\cdot(Df)_{X_0}$, all of the Lyapunov exponents can be calculated by evaluating the Jacobian of the function f along a trajectory $\{X_t\}$.

These two approaches are regarded to be qualitatively equivalent without any ambiguity. A small quantitative de-

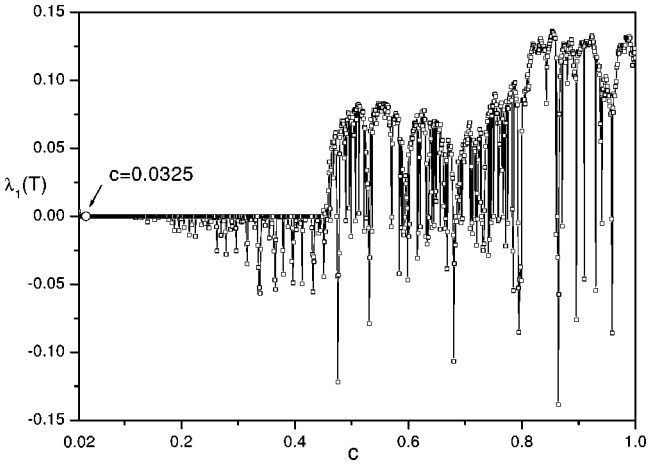

FIG. 1. $a=3.4$, $\omega=0.001\times(\sqrt{5}-1)/2$. These parameters will be used in all the following figures. Double precision (the computation error is about the order of 10^{-16}) is used in Figs. 1–5. The largest LE $\lambda_1(T)$ computed according to Eq. (2) vs c. The largest LE is zero in a large region for $c<0.045$, and the circle indicates the parameter $c=0.0325$ which will be used in all the following figures.

 ©2001 The American Physical Society

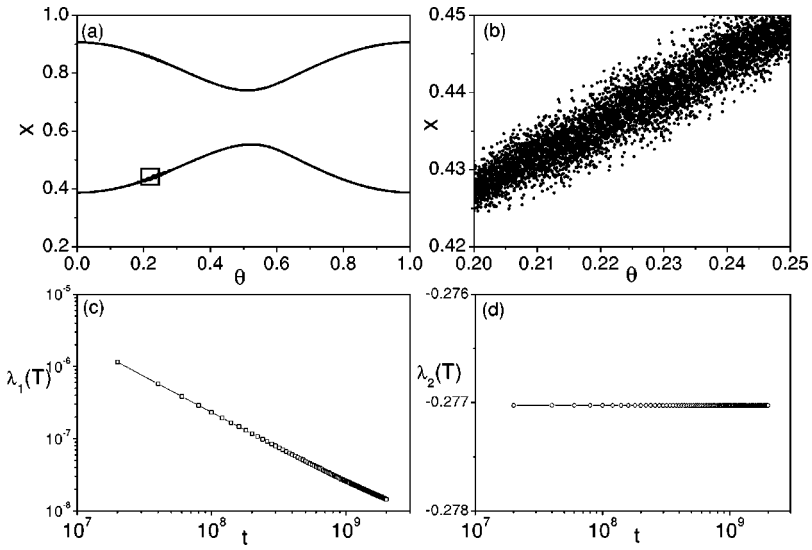

FIG. 2. $c=0.0325$. (a) The attractor of Eqs. (3). Nondifferential parts can be observed in the two branches. (b) The amplification of the marked region of (a). (c) and (d) The two LEs $\lambda_1(T)$ and $\lambda_2(T)$ of the system, computed in Eq. (2), plotted vs the average time t. (c) As t increases, the largest LE $\lambda_1(T)$ approaches zero. (d) The second LE $\lambda_2(T)$ saturates to a finite negative value.

viation may exist between $\lambda_1(D)$ and $\lambda_1(T)$ due to the choice of the initial distance of the two adjacent trajectories $(\Delta l_0(D))$ in the first method.

In this paper we consider a two-dimensional map system, which has one zero and one negative LEs, and it is nonchaotic and neither strange. Thus, this system is essentially different from the systems mentioned in the beginning. However, our system has a common feature as the previous ones that the second LE contains positive segments of local LE. We find that in certain range well above the computation error the system shows chaoslike behavior and the largest LE's computed from the above two methods are totally dif-

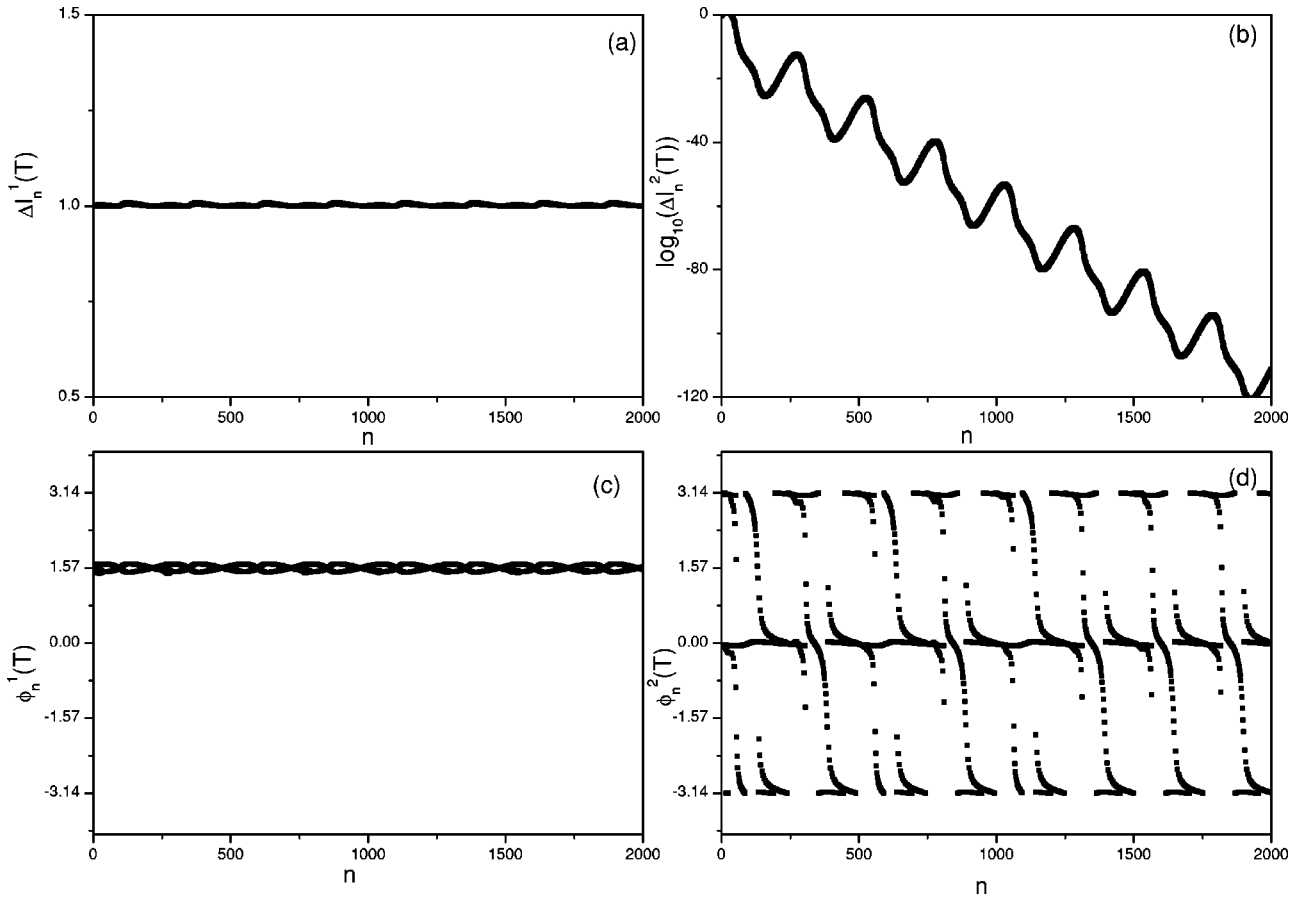

FIG. 3. (a) The variation of the length of the first mode $\Delta l_n^1(T)$, corresponding to $\lambda_1(T)$ in the tangent space. The curve oscillates around 1, confirming $\lambda_1(T)=0$. (b) The same as (a) with the second mode [for $\lambda_2(T)$] is plotted. This mode shrinks to zero eventually, indicating $\lambda_2(T)<0$. (c) The angle of the first mode, $\phi_n^1(T)$, plotted vs n. (d) The angle of the second mode, $\phi_n^2(T)$, plotted vs n.

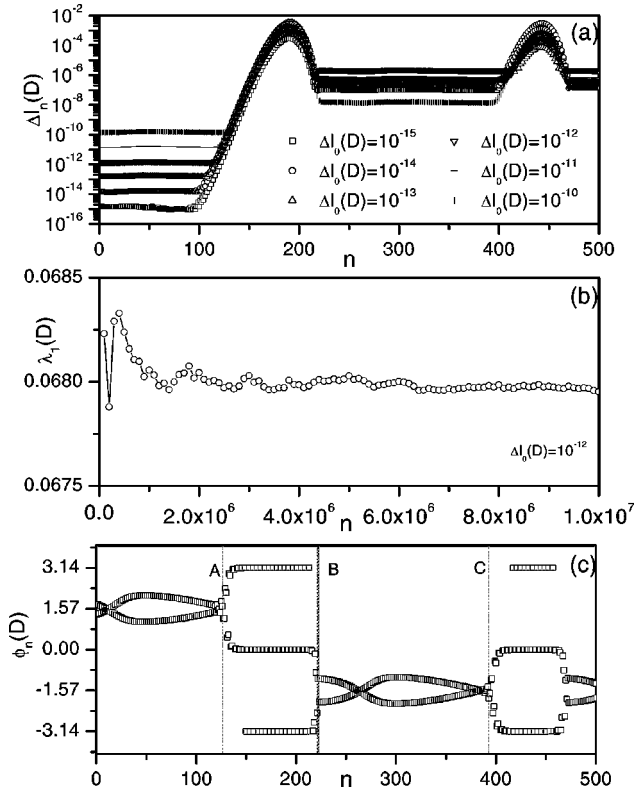

FIG. 4. (a) The variations of the distances between two adjacent trajectories. The distances increase quickly to the maximal value about the width of the nondifferential part of Fig. 2(b), disregarding the values of the initial distances. (b) The largest LE $\lambda_1(D)$ computed in Eq. (1), vs t. $\Delta l_0(D)=10^{-12}$. (c) The angle $\phi_n(D)$ defined in (5) plotted vs n. In the peaked (flat) parts of (a) the angle is 0 or π ($-\pi/2$ or $\pi/2$), which is in the direction of the second mode (first mode) in Figs. 3(b) and 3(d) [Figs. 3(a) and 3(c)].

ferent, one $[\lambda_1(D)]$ is definitely positive but the other $[\lambda_1(T)]$ is zero. It is argued that the positive segments of the local LE of the second negative LE mode and the computation error are responsible for this strange behavior, which can be typically observed in experiments with small and finite noise.

II. CHAOSLIKE BEHAVIOR IN A NONCHAOTIC MODEL SHOWN BY DOUBLE PRECISION COMPUTATION

We consider the following two-dimensional (2D) map:

$$x_{n+1}=ax_n(1-x_n)+b\cos(\theta_n), \tag{3a}$$

$$\theta_{n+1}=\theta_n+2\pi\omega+cx_n. \tag{3b}$$

This model has been investigated extensively in connection with SNA study at the zero coupling $c=0$, which corresponds to a periodically forced map or, equivalently, a quasiperiodically driven ordinary differential equation. For $c=0$ the system has obviously a zero largest LE, and the other LE may be negative for certain range of a with positive local LE as we can see for all cases of SNA [5]. It is interesting to investigate the case with nonzero coupling, which, nevertheless, has been considered much less so far.

We fix $a=3.4$, $b=0.1$, and $\omega=0.001\times(\sqrt{5}-1)/2$ and study the system dynamics for different coupling c numerically by taking double precision computation which is used in the absolute majority of current works. With small ω the system Eq. (3a) can be regarded to be driven adiabatically, and with $a=3.4$ and $b=0.1$ Eq. (3a) is in a range of period-2 state and some segments can manifest local positive LE.

First, we compute the largest LE of the system, $\lambda_1(T)$ vs c by taking the standard tangent space computation approach in Eq. (2), and plot $\lambda_1(T)$ vs c in Fig. 1 where for small c we find $\lambda_1(T)\leqslant 0$. In Fig. 2(a) we take $c=0.0325$ corresponding to zero $\lambda_1(T)$ and plot the asymptotic state in (x,θ) plane. Two thick segments are found in the two branches of the figure. In Fig. 2(b) we amplify the marked part in Fig. 2(a), and breaking of smooth torus is clearly observed. Since the largest LE is zero, this feature seems to indicate SNA. Actually, it is not as we will explain in Sec. III. In Figs. 2(c) and 2(d) we plot the two Lyapunov exponents $\lambda_1(T)$ and $\lambda_2(T)$ vs the average time t, respectively, for the state Fig.

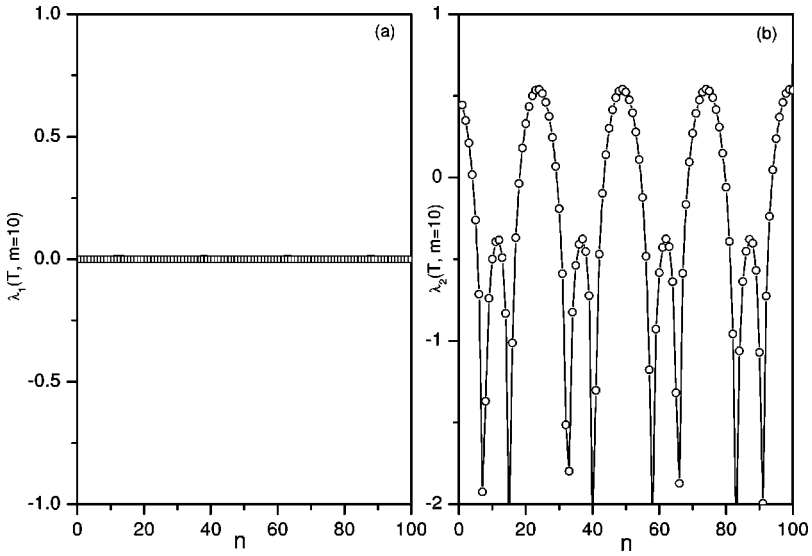

FIG. 5. Ten-step local LE for the first $[\lambda_1(T, m=10)$ (a)] and second $[\lambda_2(T,m=10)$ (b)] modes, respectively. The local LE for the first mode is about zero stably while that for the second mode varies from large positive to deep negative values. The existence of positive local LE for the second mode is the key point for the sensitive dependence of initial conditions in Fig. 4.

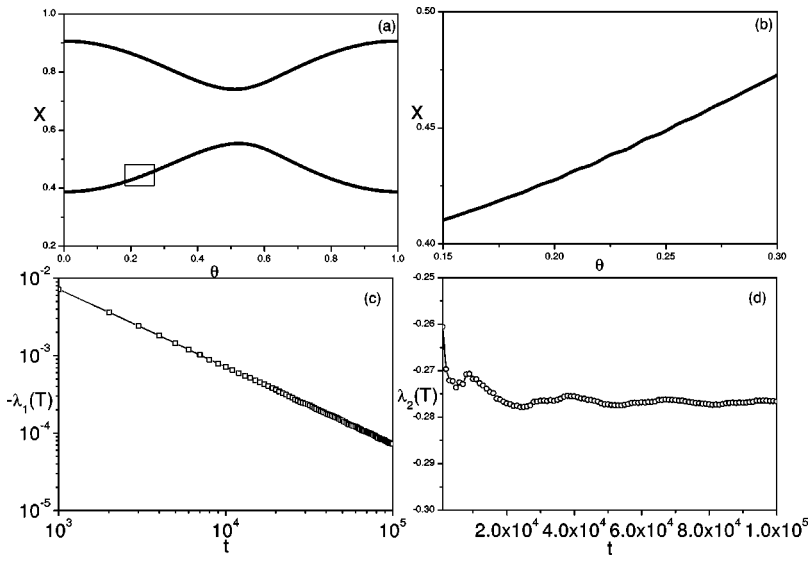

FIG. 6. The same as Fig. 2 with the computing error reduced to the order of 10^{-80}.

2(a), the plots show, without any ambiguity, zero $\lambda_1(T)$ and negative $\lambda_2(T)$. The Lyapunov exponents are obtained by applying the method based on the factorization of a matrix representation of the tangent map into a product of an orthogonal matrix Q and an upper triangular matrix R with positive diagonal elements. Such factorization can be achieved by using the Gram–Schmidt (GS) orthogonalization procedure or the QR factorization that uses the Householder transformation (HQR). The results of two methods are essentially the same [13–16]. The HQR method, which is used in our computation, is more computationally efficient and stable with regard to roundoff errors than the MGS approaches.

For clearly showing the time evolutions of the two modes $\overrightarrow{r_n^{(1)}}$ and $\overrightarrow{r_n^{(2)}}$ [corresponding to $\lambda_1(T)$ and $\lambda_2(T)$, respectively] in the tangent space, we plot in Fig. 3 the variations of the lengths $\Delta l_n^{1,2}(T)$ and the angles $\phi_n^{1,2}(T)$ of $\overrightarrow{r_n^{(1)}}$ and $\overrightarrow{r_n^{(2)}}$ vs the iteration time n, where $\Delta l_n^{1,2}(T)$ and $\phi_n^{1,2}(T)$ are defined as

$$\Delta l_n^{1,2}(T)=\sqrt{(\Delta\theta_n^{1,2}(T))^2+(\Delta x_n^{1,2}(T))^2},$$
$$tg(\phi_n^{1,2}(T))=\Delta\theta_n^{1,2}(T)/\Delta x_n^{1,2}(T). \tag{4}$$

The superscripts 1 and 2 represent the mode index, $\Delta\theta_n^{1,2}(T)$ and $\Delta x_n^{1,2}(T)$ are the coordinates of the mode $\overrightarrow{r_n^{(1)}}$ and $\overrightarrow{r_n^{(2)}}$, respectively. In our computation, we first neglect a transient of 10^4 iterations and then normalize $\Delta l_0^{1,2}(T)=\sqrt{\Delta\theta(T)^2+\Delta x(T)^2}=1$ for both modes for the first computation iteration. In Figs. 3(a) and 3(b) the lengths of the first and the second modes are plotted, respectively. The length of the first mode oscillates around 1 all the time, corresponding to zero LE. The second mode eventually shrinks to zero, reasonably indicating negative LE. In Figs. 3(c) and 3(d) the angles of the two modes are plotted, it is interesting to notice that the first mode fluctuates always along the θ axis (say, with angle $\pi/2$ or $-\pi/2$), while the second one varies along the x axis basically (with angle 0 or π). These are reasonable since at $c=0$ the first and the second modes are exactly along the axis θ and x axis, respectively, and the small nonzero coupling c can induce some small fluctuations of the modes along these directions only.

All the results in Figs. 1, 2(c), 2(d), and 3 are obtained through the computation in the tangent space. For understanding the nature of the distribution Fig. 2(b) we directly calculate the evolution of a small difference between two adjacent trajectories of the system (3). Suppose two trajectories (x_n,θ_n) and (x_n',θ_n') are close to each other initially, their difference vector $\overrightarrow{\Delta l_n}$ has its length and angle as

$$\Delta l_n(D)=\sqrt{(\Delta\theta_n(D))^2+(\Delta x_n(D))^2},$$
$$tg(\phi_n(D))=\Delta\theta_n(D)/\Delta x_n(D),$$
$$\Delta\theta_n(D)=\theta_n-\theta_n',\quad \Delta x_n(D)=x_n-x_n'. \tag{5}$$

In Fig. 4(a) we plot $\Delta l_n(D)$ vs n for different initial $\Delta l_0(D)$. For each $\Delta l_0(D)$ we find $\Delta l_n(D)$ quickly increases [note, in Fig. 4 $\Delta l_n(D)$ is no longer reset to $\Delta l_0(D)$ after each iteration] to a distance $\Delta l_n(D)\approx 0.01$, which is nothing but the width of the attractor in the nondifferential segments [see Fig. 2(b)]. For having the expanding rate of Fig. 4(a), the LE averaged in a long time period [i.e., $\lambda_1(D)$] should be of the order 0.1 as we can see in Fig. 4(b), which is in a striking contrast to the zero largest LE $\lambda_1(T)$ of Fig. 2(c) and zero expansion rate of the tangent vector in Fig. 3(a).

An interesting question is how the expansions of Fig. 4(a) can occur in a dynamic system of which no expansion exists in all directions of the tangent space in the average sense [see Figs. 2(c), 2(d), 3(a), and 3(b)]. For answering this question, we first plot $\phi_n(D)$ vs n in Fig. 4(c), where we find that $\phi_n(D)$ jumps between two sets of angles 0 or $\pi \rightleftharpoons -\pi/2$ or $\pi/2$. In Figs. 3(c) and 3(d) we have already shown that $-\pi/2,\pi/2$, and $0,\pi$ correspond to the mode directions of zeros (the largest) and negative LEs, respectively. Thus, the difference vector $\overrightarrow{\Delta l_n}$ jumps between the directions of the two modes. Comparing Fig. 4(c) with 4(a) we find that the

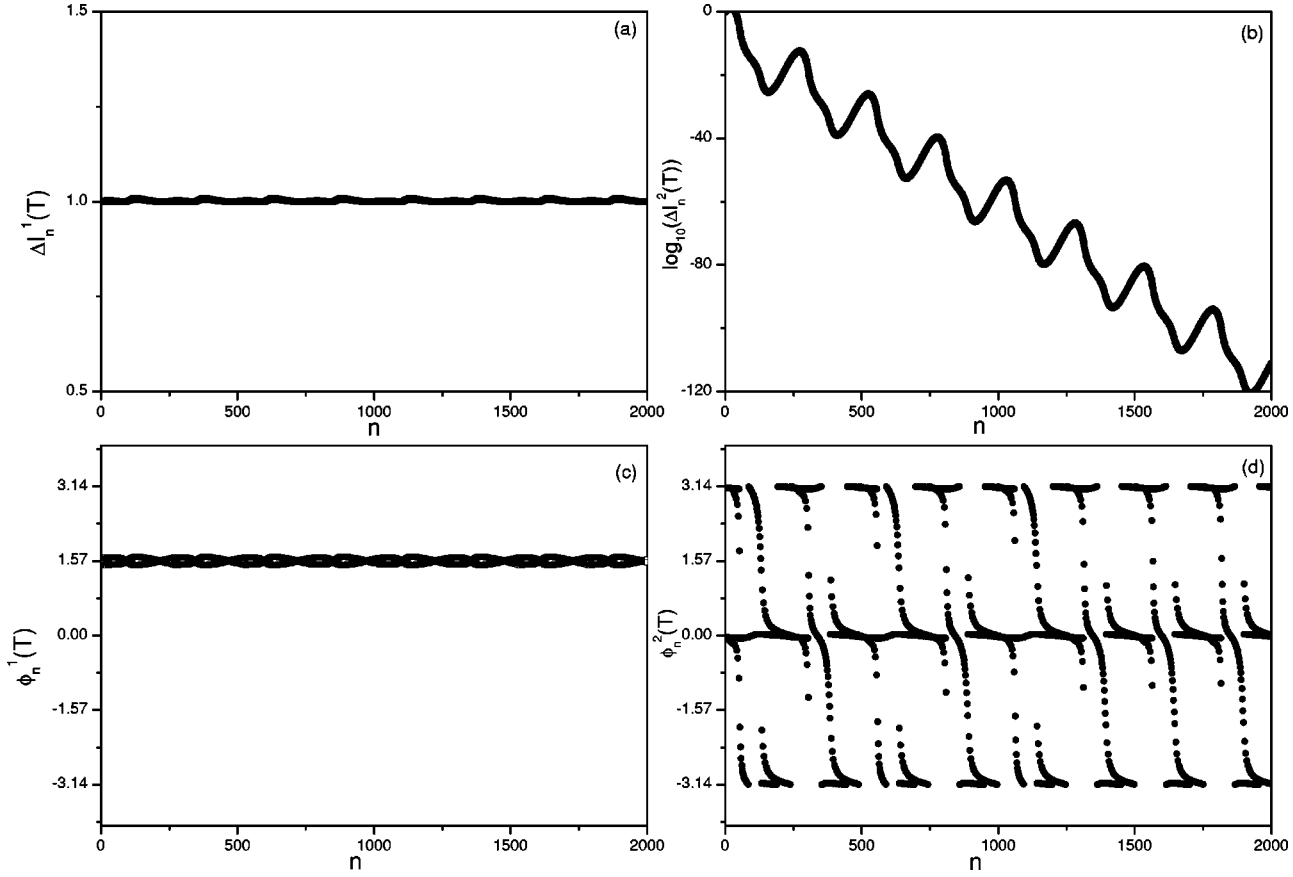

FIG. 7. The same as Fig. 3 with the computing error reduced to the order of 10^{-80}.

expansion of $\Delta l_n(D)$ in Fig. 4(a) occurs always when $\overrightarrow{\Delta l_n}$ has angle $\phi_n(D) \approx 0$ or π, i.e., when $\overrightarrow{\Delta l_n}$ is in the direction of the second (negative LE) mode, while $\Delta l_n(D)$ curve becomes flat in the region of $\phi_n(D) \approx -\pi/2$ or $\pi/2$, i.e., in the direction of the first (zero LE) mode. Jumps from $-\pi/2$, $\pi/2$ angle (0, π angle) to 0, π angle ($-\pi/2$, $\pi/2$ angle) in Fig. 4(c) correspond to the turnings from the flat (peaked) segments to the peaked (flat) segments in Fig. 4(a), this explains why $\lambda_1(D)$ is different from $\lambda_1(T)$ computed in the tangent space.

In order to understand why $\overrightarrow{\Delta l_n}$ expands in the direction of the second mode (the mode of negative LE) we investigate the local LEs for both $\lambda_1(T)$, $\lambda_2(T)$ modes. In Figs. 5(a) and 5(b) we plot the 10 step local LEs for the first and the second modes vs the iteration time *n*, respectively. By *m* step local LE we mean

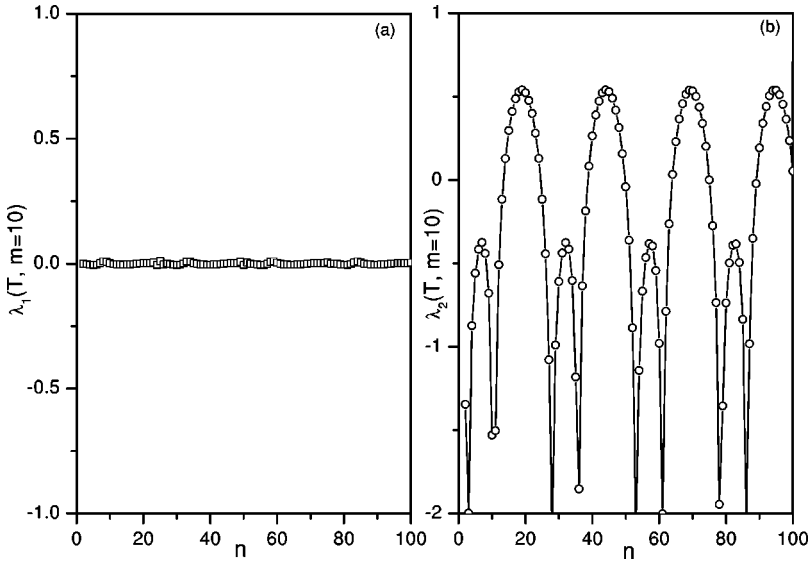

FIG. 8. The same as Fig. 5 with the computing error reduced to the order of 10^{-80}.

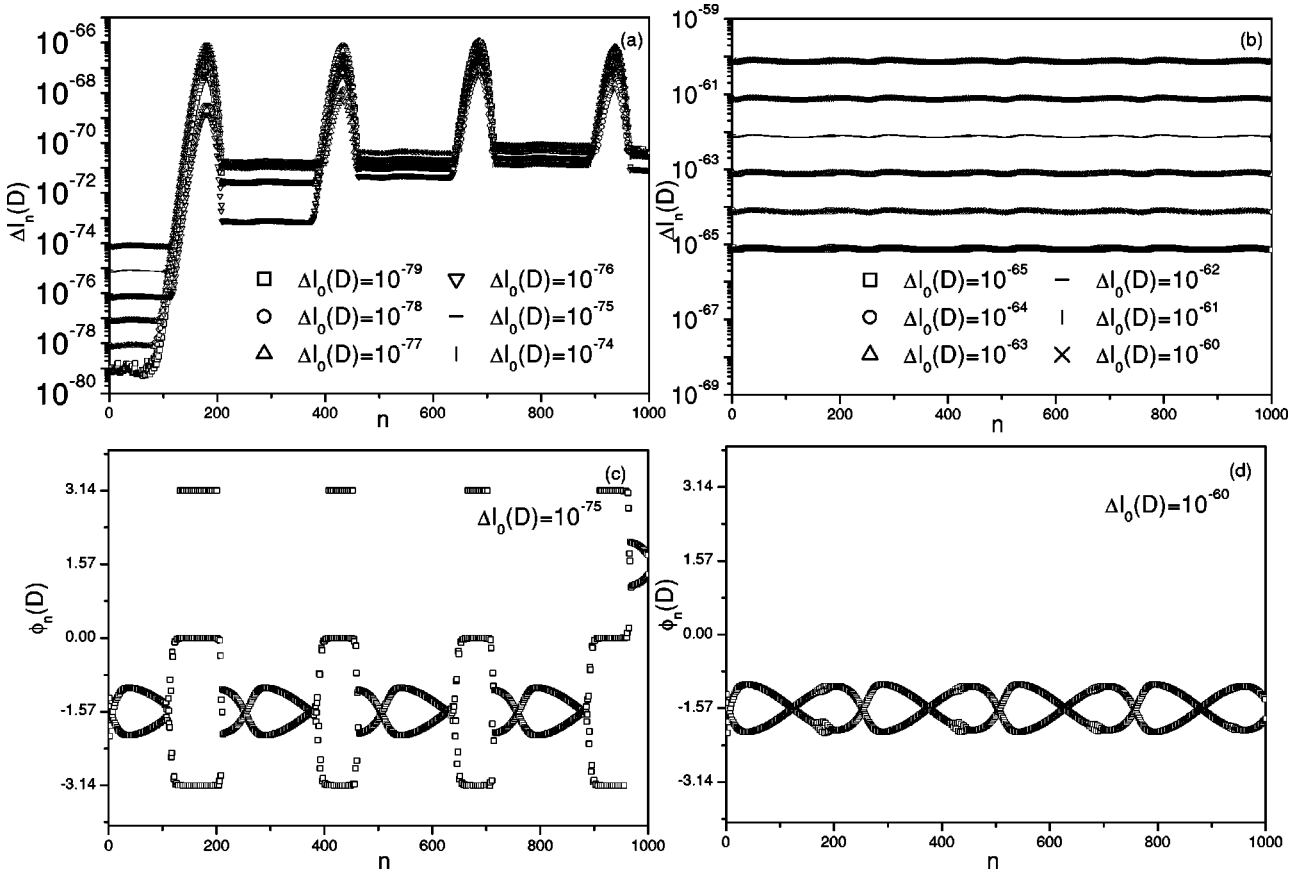

FIG. 9. (a) and (b) The same as Fig. 4(a) with the computing error 10^{-80}. Note the different values of $\Delta l_0(D)$ in both figures. (c) and (d) The same as Fig. 4(c) with the computing error 10^{-80} and with different $\Delta l_0(D)$.

$$\lambda_j(T,m,n)=\frac{1}{m}\ln\|(Df^m)_{X_n}\cdot v\|, \tag{6}$$

where $(Df)^m_{X_n}=(Df)_{X_{n+m-1}}\cdot(Df)_{X_{n+m-2}}\cdots(Df)_{X_n}$, and all the notations have the same meanings as in Eq. (2) except the infinite average time from $n=1$ to $t\to\infty$ in (2) is replaced by a finite time average from n to $n+m-1$.

For computing the m step local LE we again neglect the first 10^4 iterations for avoiding the transient effect. The first local LE $\lambda_1(T,\ m=10)$ in Figs. 5(a) is approximately zero with small fluctuations around. Large positive and negative values can appear in some segments of Figs. 5(b) for the second local LE $\lambda_2(T,\ m=10)$ though the long time average of the second LE $\lambda_2(T)$ is definitely negative, and the positive segments of the second local LE $\lambda_2(T,\ m=10)$ are in accordance with the regions in Fig. 4(a) where $\Delta l_n(D)$ rapidly raises. Now the sensitive initial value dependence of Fig. 4 can be well understood, based on the two local LEs $\lambda_{1,2}(T,\ m)$ of Fig. 5 and the jumping behavior of Fig. 4(c).

Given any two adjacent trajectories (x_n,θ_n) and (x'_n,θ'_n), the distance vector between them, $\overrightarrow{\Delta l}_n$, must contain both $\overrightarrow{r_n^{(1)}}$ and $\overrightarrow{r_n^{(2)}}$ modes. As the trajectories enter the segments with large positive local second LE, $\overrightarrow{\Delta l}_n$ increases exponentially, producing a raising part of Fig. 4(a), and $\overrightarrow{\Delta l}_n$ takes the direction of $\overrightarrow{r_n^{(2)}}$ as shown in Fig. 4(c). As the trajectories pass this unstable time region [see the AB segment in Fig. 4(c)] and enter the interval with negative local LE, $\overrightarrow{r_n^{(2)}}$ shrinks and so does $\overrightarrow{\Delta l}_n$, this yields the part BC in Fig. 4(c) where $\overrightarrow{r_n^{(1)}}$ dominates in $\overrightarrow{\Delta l}_n$, and $\Delta l_n(D)$ maintains nearly a constant value. The similar process repeats in each circle during the evolution of the system, and yield the result of Fig. 4.

In summary, we find a chaoslike behavior [see the seemly strange attractor in Fig. 2(b) and the positive $\lambda_1(D)$] in a nonchaotic system [$\lambda_{1,2}(T)\leqslant 0$]. In the next section it will be clear that this chaoslike behavior is caused by the computation precision and the second local positive LE.

III. NUMERICAL RESULTS BY HIGH-PRECISION COMPUTATION

In order to thoroughly understand the strange behavior in Sec. II, we conduct numerical simulation by applying high-precision computation, namely, using the Maple VI algorithm.

In Fig. 6 we do exactly the same as Fig. 2 except using computation precision 10^{-80} (note, the double precision is about 10^{-16}). It is noticed that the size of the width of the nondifferential part in Fig. 2 is greatly shrinking in Fig. 6 from the order 10^{-2} to the order 10^{-66} [invisible in Figs. 6(a) and 6(b)], the difference between these orders is pre-

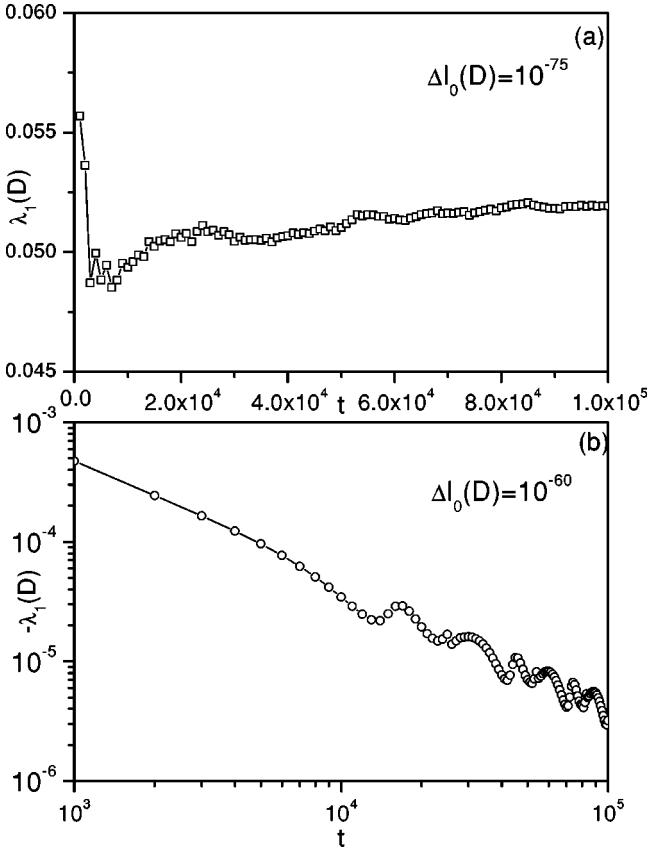

FIG. 10. (a) and (b) The same as Fig. 4(b) with $\Delta l_0(D)$ replaced by 10^{-75} and 10^{-60}, respectively. The computing error is of order 10^{-80}.

cisely the same as the difference of the orders for the corresponding computation precisions. This shrinking shows that the strange behavior in Fig. 2(b) is caused by the computation errors amplified by the local positive LE of the second mode. However, the two LEs $\lambda_1(T)$ and $\lambda_2(T)$ in Figs. 6(c) and 6(d) are not changed from Figs. 2(c) and 2(d), that indicates the results computed in the tangent space are not apparently affected by different computation precisions. This conclusion is further confirmed by Figs. 7 and 8 where we do exactly the same as Figs. 3 and 5 by replacing the double precision by the precision of 10^{-80}, there is nothing essentially changed in Figs. 7 and 8 from Figs. 3 and 5, respectively.

In Figs. 9(a) and 9(b) we do the same as Fig. 4(a) with 10^{-80} precision applied. The evolutions of various $\Delta l_n(D)$ sequences depend on their initial distance $\Delta l_0(D)$. For $\Delta l_0(D)$ considerably smaller than 10^{-66} [Fig. 9(a)] we find the same behavior as Fig. 4(a) except the maximal value of $\Delta l_n(D)$ can go up only to 10^{-66}, which is nothing but the width of the nondifferential region of Fig. 6(b) (invisible), and is 10^{14} larger than the computation precision [in Fig. 4(a) this ratio is also about 10^{14}]. However, for $\Delta l_0(D)$ much larger than 10^{-66}, in Fig. 9(b) $\Delta l_n(D)$ is practically unchanged after the transient, and no sensitivity of the system motion to the initial value can be observed, this is well in accordance with the zero largest LE of Fig. 6(c). In Figs. 9(c) and 9(d) we plot the angle $\phi_n(D)$ of $\vec{\Delta l}_n$ for $\Delta l_0(D)$

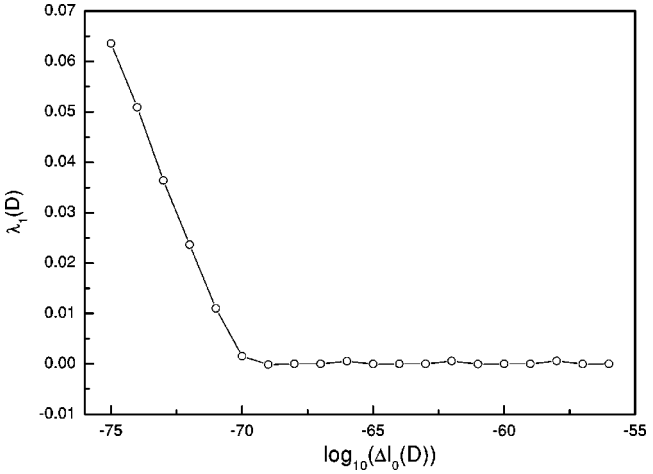

FIG. 11. $\lambda_1(D)$ plotted vs $\Delta l_0(D)$. The computing error is of order 10^{-80}.

$=10^{-75}$ and 10^{-60}, respectively. In Fig. 9(c) $\phi_n(D)$ jumps among the directions of the first ($\pm\pi/2$) and the second (0, $\pm\pi$) modes, corresponding to the flat and peaked segments of Fig. 9(a), respectively , while in Fig. 9(d) $\phi_n(D)$ keeps in the direction ($\pm\pi/2$) of the first mode [zero $\lambda_1(T)$ mode], and this explains the nearly constant $\Delta l_n(D)$ in Fig. 9(b).

With the computation precision 10^{-80}, we can calculate $\lambda_1(D)$ of Eq. (1) by varying $\Delta l_0(D)$ in a large scale. In Fig. 10(a) we take $\Delta l_0(D)=10^{-75}$ which is much smaller than the width of the nondifferential region in Fig. 6(b) and plot $\lambda_1(D)$ vs the average time t, $\lambda_1(D)$ approaches to a finite positive value (about 0.052) obviously in agreement with the variation $\vec{\Delta l}_n$ in Figs. 9(a) and 9(c). In Fig. 10(b) we take $\Delta l_0(D)=10^{-60}$, which is considerably larger than the corresponding region width, and the $\lambda_1(D)$ approaches zero as t increases, this is expected from the evolution of $\vec{\Delta l}_n$ in Figs. 9(b) and 9(d). In Fig. 11 $\lambda_1(D)$ is plotted against $\Delta l_0(D)$, positive $\lambda_1(D)$ is obviously observed in the region $\Delta l_0(D)$ $<10^{-70}$ and zero $\lambda_1(D)$ is identified for $\Delta l_0(D)>10^{-66}$.

IV. CONCLUSION

In conclusion a chaoslike behavior in nonchaotic systems can be observed for a certain range of detection if some local Lyapunov exponent of a negative LE is positive. By nonchaotic system we mean that all the LEs computed in the tangent space [Eq. (2)] are nonpositive; by chaoslike behavior we mean the attractor contains nondifferential parts and the motion is sensitive to the initial condition. The range where this strange behavior appears depends on the numerical computation error and the expanding rate of the local positive LE. More specifically, this range is between $10^{-\alpha}$ and $10^{\beta-\alpha}$ where $10^{-\alpha}$ is the order of computation error and 10^{β} is the expansion rate in a positive local Lyapunov exponent segment of the corresponding mode of negative LE. Well above this range the attractor is smooth and the motion is regular.

A practically interesting point is that the above range for chaoslike behavior can be easily observed in numerical computations or in experiments if the expansion rate is large as

$\beta \approx \alpha$. For instance, in our model we have $\beta \approx 14$, and then this ''chaotic behavior'' becomes inevitable when the double precision $\alpha \approx 16$, which is extensively applied in the current numerical works, is used. In order to make the numerical simulation convincing in these cases we have to reduce the computation error (increase α). However, if the same problem ($\alpha \approx \beta$) occurs in experiments with noise of $10^{-\alpha}$ intensity, the chaoslike behavior in nonchaotic systems shown in Sec. II becomes inevitable and typical in reality.

A point of conceptional significance is related to the computation of the largest LE. It is found that the LEs computed in the tangent space [$\lambda_1(T)$ in Eq. (2)] are not sensitive to the computation precision. However, the largest LE, computed in Eq. (1), $\lambda_1(D)$, based on the distance of adjacent trajectories, sensitively depends on the choice of the distance $\Delta l_0(D)$, if some negative LE mode has positive local LE segment. Correct $\lambda_1(D)$ [i.e., $\lambda_1(D)=\lambda_1(T)$] can be obtained only if $\Delta l_0(D)$ much smaller than the attractor size and well above the range $10^{\beta-\alpha}$. So far in applying Eq. (1) only the condition $\Delta l_0(D) \ll 1$ (suppose the attractor size is of order 1) has been required for guaranteeing the validity of linearization. Now we find that $\Delta l_0(D)$ should be restricted by a lower threshold if some negative LE modes have positive local LE such as $\Delta l_0(D) > 10^{\beta-\alpha}$. If β is large this lower limit may be up to the order of the trajectory size, then the approach of Eq. (1) fails.

As $\Delta l_0(D)$ in Eq. (1) is in between $10^{-\alpha}$ and $10^{\beta-\alpha}$ we can obtain positive $\lambda_1(D)$ when $\lambda_1(T)=0$, corresponding to the chaoslike behavior in a nonchaotic system. For instance, we take $\Delta l_0(D)=10^{-75}$ in Fig. 10(a), which is much larger than the computing error and much smaller than the attractor size. According to the conventional point of view, in this case the $\lambda_1(D)$ in (1) should be practically the same as $\lambda_1(T)$ in (2), since linearization around the trajectory is well satisfied and the computing error is too small to affect the $\lambda_1(D)$ value. However, we still have positive $\lambda_1(D)$ in Fig. 10(a), the same behavior can be seen in Fig. 4(b) and Fig. 11 for $\Delta l_0(D) < 10^{-70}$. The intuitive picture for the positivity of $\lambda_1(D)$ is the following: suppose in our case $\vec{r_n^{(1)}}$ and $\vec{r_n^{(2)}}$ are the two vector modes, corresponding to the LEs $\lambda_1(T)=0$, $\lambda_2(T)<0$, respectively. The length $|\vec{r_n^{(1)}}|=\Delta l_n^1(T)$ practically maintains a constant value while $|\vec{r_n^{(2)}}|=\Delta l_n^2(T)$ expands in the time interval when local LE $\lambda_2(T)$ is positive and shrinks when local LE $\lambda_2(T)$ is negative. For long time average $\Delta l_n^1(T)$ is a constant value while $\Delta l_n^2(T)$ contracts to zero. When we compute $\lambda_1(D)$ in Eq. (1) with $\Delta l_0(D)$ being in the region $10^{-\alpha} < \Delta l_0(D) < 10^{\beta-\alpha}$, we can find $\vec{\Delta l_n}$ takes $\vec{r_n^{(1)}}$ direction when $\Delta l_n^2(T)$ shrinks and takes $\vec{r_n^{(2)}}$ direction when $\Delta l_n^2(T)$ expands, i.e., $\vec{\Delta l_n}$ has an intention to take the direction of the most expanding (or say, least contracting) mode, that produces positive $\lambda_1(D)$ while $\lambda_1(T)=0$. For having $\lambda_1(D) > \lambda_1(T)$, it is important that the second negative LE mode has positive local LE. This inconsistence would not appear if the local positive LE appears in the first zero mode. For instance, if we neglect the coupling in Eq. (3), $c=0$, the $\lambda_1(D)$ computed in Eq. (1) will never be positive [we will have $\lambda_1(D)=\lambda_1(T)=0$ or $\lambda_1(D)=\lambda_2(T)<0$, depending on the length order of $\Delta l_0(D)$] for arbitrary $\Delta l_0(D) > 10^{-\alpha}$ although β is still very large in this uncoupled case.

ACKNOWLEDGMENTS

This research is supported by the National Natural Science Foundation of China, the Nonlinear Science Project of China, and the Foundation of Doctoral training of Educational Bureau of China.

[1] J. P. Eckmann and D. Ruelle, Rev. Mod. Phys. **57**, 617 (1985).
[2] G. Benettin, L. Galgani, A Giorgilli, and J.-M. Strelcyn, Meccanica **15**, 21 (1980).
[3] J. L. Kaplan and J. A. Yorke, Commun. Math. Phys. **67**, 93 (1979).
[4] E. Ott, *Chaos in Dynamical Systems* (Cambridge University Press, Cambridge, England, 1994).
[5] A. S. Pikovsky and U. Feudel, Chaos **5**, 253 (1995).
[6] S. Kuznetsov, E. Neumann, A. Pikovsky and I. R. Sataev, Phys. Rev. E **62**, 1995 (2000).
[7] R. Bowen, J. Differential, J. Diff. Eqns. **18**, 333 (1975).
[8] S. M. Hammel, J. A. York, and C. Grebogi, Bull. Am. Math. Soc. **19**, 465 (1988).
[9] C. Grebogi, S. M. Hammel, J. A. York, and T. Sauer, Phys. Rev. Lett. **65**, 1527 (1990).
[10] S. Dawson, C. Grebogi, T. Sauer, and J. A. York, Phys. Rev. Lett. **73**, 1927 (1994).
[11] J. M. Sanz-Serna and S. Larsson, Appl. Numer. Math. **13**, 181 (1993).
[12] T. Sauer, C. Grebogi, and S. M. Hammel, Phys. Rev. Lett. **79**, 59 (1997).
[13] H. F. von Bremen, F. E. Udwadia, and W. Proskurowski, Physica D **101**, 1 (1997).
[14] A. Wolf, J. B. Swift, H. L. Swinney, and J. A. Vastano, Physica D **16**, 285 (1985).
[15] J. M. Greene and J.-S. KIM, Physica D **24**, 213 (1987).
[16] K. Ramasubramanian and M. S. Sriram, Physica D **139**, 72 (2000).